Collaborative Honeypot Defense in UAV Networks: A Learning-Based Game Approach

Yuntao Wang[†], Zhou Su[†], Abderrahim Benslimane[‡], Qichao Xu[¶], Minghui Dai[§], and Ruidong Li[‡‡]

[†]School of Cyber Science and Engineering, Xi'an Jiaotong University, China

[‡]Laboratory of Computer Sciences, Avignon University, France

[¶]School of Mechatronic Engineering and Automation, Shanghai University, China

[§]State Key Laboratory of Internet of Things for Smart City, University of Macau, Macau, China

[‡‡]Department of Electrical and Computer Engineering, Kanazawa University, Japan

Abstract—The proliferation of unmanned aerial vehicles (UAVs) opens up new opportunities for on-demand service provisioning anywhere and anytime, but also exposes UAVs to a variety of cyber threats. Low/medium interaction honeypots offer a promising lightweight defense for actively protecting mobile Internet of things, particularly UAV networks. While previous research has primarily focused on honeypot system design and attack pattern recognition, the incentive issue for motivating UAV's participation (e.g., sharing trapped attack data in honeypots) to collaboratively resist distributed and sophisticated attacks remains unexplored. This paper proposes a novel game-theoretical collaborative defense approach to address optimal, fair, and feasible incentive design, in the presence of network dynamics and UAVs' multi-dimensional private information (e.g., valid defense data (VDD) volume, communication delay, and UAV cost). Specifically, we first develop a honeypot game between UAVs and the network operator under both partial and complete information asymmetry scenarios. The optimal VDD-reward contract design problem with partial information asymmetry is then solved using a contract-theoretic approach that ensures budget feasibility, truthfulness, fairness, and computational efficiency. In addition, under complete information asymmetry, we devise a distributed reinforcement learning algorithm to dynamically design optimal contracts for distinct types of UAVs in the time-varying UAV network. Extensive simulations demonstrate that the proposed scheme can motivate UAV's cooperation in VDD sharing and improve defensive effectiveness, compared with conventional schemes.

Index Terms—Unmanned aerial vehicle (UAV), mobile honeypot, collaborative defense, game, reinforcement learning.

I. INTRODUCTION

With the advancements in communication and embedded technologies, unmanned aerial vehicles (UAVs) have been widely employed in a variety of applications including power lines inspection, medical delivery, disaster search, and crowd surveillance [1]–[3]. Thanks to their low cost, 3D mobility, and flexible deployment, UAVs can be swiftly dispatched to hard-to-reach sites (e.g., disaster zones) to undertake time-critical missions and offer urgent communication services using line-of-sight (LoS) links [4]–[6]. As UAVs are computer-controlled agents with wireless/radio interfaces, the widespread use of UAVs in service offering exposes them to a plethora of sophisticated cyber attacks [7] such as eavesdropping, hijacking, data theft, and denial-of-service (DoS).

In the face of escalating cyber threats, low/medium-interaction honeypots, as a supplemental active defense tech-

nology, provide a cost-effective alternative to strengthen UAV defense [8]–[10]. Honeypots are physical or virtual systems that imitate real devices to lure and trap intruders, allowing defenders to continuously learn new attack patterns [11]. Low/medium-interaction honeypots (which simulate network operations on the TCP/IP stack) can provide lightweight defenses, compared to resource-hungry high-interaction honeypots [10], [12]. These defenses are particularly suitable for mobile and resource-constrained devices (such as battery-powered UAVs), which have drawn numerous research efforts. For example, Vasilomanolakis *et al.* [13] develop the HosTaGe prototype, a generic low-interaction honeypot, for mobile devices to identify fraudulent wireless networks as they connect. Meanwhile, a medium-interaction honeypot prototype called HoneyDrone is implemented on small-size UAVs by Daubert *et al.* [14] via simulating UAV-specific protocols in the UAV honeypot.

Despite the fundamental contributions to system and software design of existing literature [13], [14], the honeypot-based cooperative defensive strategy for UAVs is rarely studied. Particularly, given the current trend of distributed, sophisticated, and complex covert cyber attacks (e.g., advanced persistent threat (APT) and distributed DoS (DDoS)), there is a necessity for large-scale collaborative defense among UAVs for global situational awareness by exchanging trapped attack information (e.g., attack interaction logs) in local honeypots. Nonetheless, as participating in such collaboration mechanisms entails significant costs (e.g., honeypot execution and communication costs) and potential privacy leakage (e.g., UAV configuration and flying route), UAVs might be reluctant to share their captured attack data without adequate incentives. Additionally, malicious UAVs may distribute false attack information to mislead others. Therefore, it is imperative to design an effective incentive mechanism to encourage UAVs to honestly cooperate in the joint defense.

However, the following key challenges need to be resolved to design such an incentive mechanism compatible with UAVs. First, UAVs typically have multi-dimensional private information in terms of valid defense data (VDD) volume, communication delay, VDD cost, and privacy cost. Moreover, selfish UAVs may launch free-riding attacks, namely, they will not contribute to but still benefit from the joint defense, thereby disincentivizing honest UAVs. The presence of UAV's multi-
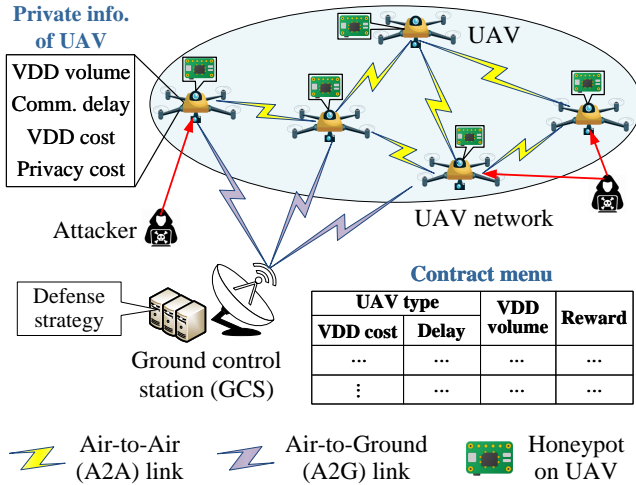
Fig. 1. Illustration of the incentive-driven honeypot game for collaborative defense via sharing VDD in UAVs' local honeypots.

dimensional information asymmetry and free-riding behaviors poses significant challenges in *optimally* and *fairly* distributing rewards to compensate for UAV costs. Besides, as both UAV networks and attack behaviors can be highly dynamic, the shared defense data from UAVs should be timely aggregated to produce real-time defense strategies. As such, it remains a challenge to *feasibly* implement the incentive mechanism in practical UAV applications with time-varying environments and stringent latency requirements.

To address these issues, this paper proposes a novel incentive-driven honeypot-based collaborative UAV defense scheme to enhance defensive effectiveness, in which optimal, fair, and feasible incentives are offered to promote UAVs' honest cooperation in the face of information asymmetry and network dynamics. Firstly, we present a UAV honeypot game framework consisting of multiple UAVs and a ground control station (GCS) serving as the network operator. In the game, as shown in Fig. 1, the GCS designs a series of contracts (specifying the relation among VDD size, VDD cost, communication delay, and rewards) for heterogeneous UAVs, and each UAV chooses a contract to share its defense data. Then, we formulate the optimal contract design problem for GCS under practical constraints and different levels of information asymmetry. Next, by leveraging the revelation principle, we analytically derive the optimal contract under *partial information asymmetry* (i.e., GCS knows the numbers of different types of UAVs) and rigorously prove its truthfulness, fairness, budget feasibility (BF), and computational efficiency. Furthermore, under *complete information asymmetry* (i.e., GCS only knows the number of UAVs), we develop a two-tier reinforcement learning (RL) algorithm to dynamically acquire optimal contracts for different types of UAVs via trials with high adaption to the fast-changing network environment.

The main contribution of this work is three-fold as below.

- *Honeypot game theoretical cooperative defense framework*. We propose an active and cooperative defense framework based on honeypot game to encourage distributed UAVs to share honeypot data with the defensive

designer (i.e., GCS). Under this framework, feasible incentive mechanisms are designed to forbid free-riding UAVs while ensuring compensation fairness and optimality under different levels of information asymmetry.

- *Budget-constrained optimal contract design under partial information asymmetry*. We leverage the multi-dimensional contract theory to design optimal fair contracts for heterogeneous UAVs with multi-dimensional private types under partial incomplete information. By summarizing UAV's multi-dimensional private type into a one-dimensional criterion, the optimal data-payment contract is theoretically solved. Besides, an adaptive dynamic assignment algorithm is designed for practical deployment under budget constraints.

- *RL-based optimal contract design under complete information asymmetry*. By formulating UAVs' and GCS's interactions as finite Markov decision processes (MDPs), we devise the distributed policy hill-climbing (PHC) algorithm with two tiers to dynamically learn the optimal contractual strategies of all participants under strongly incomplete information. A hotbooting method is also designed in PHC learning to accelerate convergence rate by initializing the Q-values and mixed-strategy tables using historical experience.

- *Extensive simulations for performance evaluation*. We evaluate the efficiency and effectiveness of the proposed scheme using extensive simulations. Numerical results show that the proposed scheme can effectively defend against free-riders and motivate UAVs' participation in honeypot defense with improved UAV utility and defensive effectiveness in both partial and complete information asymmetry scenarios, in comparison to conventional approaches.

The remainder of the paper is organized as follows. Section II reviews the related works. Section III introduces the system model and Section IV formulates the honeypot game-based cooperative defense framework. Section V designs the optimal contract under complete information. Section VI and Section VII present contract-based and RL-based optimal incentive mechanisms under partial and complete information asymmetry scenarios, respectively. Performance evaluation is given in Section VIII and conclusions are drawn in Section IX.

II. RELATED WORKS

In this section, we review the related literature on honeypot-based defenses in the Internet of things (IoT) and UAV networks, as well as game modeling for honeypot-based defense.

A. Honeypot-Based Defenses in IoT and UAV Networks

Honeypot offers an active line of defense for the IoT and mobile UAV networks by trapping and deceiving cyber attackers via carefully monitored unprotected systems. The level of interaction with adversaries can be used to classify honeypots [10]. High-interaction honeypots are real hosts or virtual machines (VMs) that replicate all of the functionalities of a real system, which are resource-hungry and typically expensive to maintain. While low/medium-interaction honeypots

TABLE I
EXISTING REPRESENTATIVE GAME-THEORETICAL HONEYPOT DEFENSE APPROACHES: A COMPARATIVE SUMMARY

Ref.	Scenario	Mobile honeypot	User's private info.		Budget feasibility	Partial & complete information asymmetry scenarios
			cost	delay		
[10]	$N.A.$	×	✓	×	×	×
[15]	Industrial IoT	×	✓	$N.A.$	×	×
[16]	Power grid	×	✓	$N.A.$	×	×
[17]	Power grid	×	✓	×	×	×
[18], [19]	General IoT	×	✓	×	×	×
[20]	Cloud computing	×	✓	$N.A.$	×	×
Ours	UAV network	✓	✓	✓	✓	✓

only simulate the networking stack at a low/high granularity to provide detailed logging and monitoring functionalities, which are much cheaper to maintain and better suited for mobile devices (e.g., UAVs) [13], [14]. Fan *et al.* [21] present a novel all-round high-interaction honeypot system to efficiently acquire high-quality attack data in the large-scale IoT. By decoupling the honeypot functions, they design an active defense mechanism by integrating the decoy module, the coordinator module, and the captive module. Its performance is validated using real deployment and tests in a software-defined environment. Based on software-defined network (SDN) and network function virtualization (NFV), Zarca *et al.* [22] design a virtual IoT honeypot network to realize flexible and programmable honeypot deployment and dynamic security policy enforcement for mitigated network attacks. Wang *et al.* [12] propose a hybrid IoT honeypot architecture for malware defense, which consists of a high-interactive component in real IoT devices and a low-interactive component in VMs with Telnet/SSH services. For small-size and mobile UAVs, Daubert *et al.* [14] develop a low/medium-interaction honeypot prototype system named HoneyDrone based on Raspberry Pi, where UAV-specific protocols are simulated in the honeypot to cheat attackers.

One can observe that existing literature mainly focuses on system architecture and protocol design for honeypots in the IoT and UAV networks, whereas the collaborative honeypot-based UAV defense mechanisms are topics that are understudied. Given the widespread, advanced, and covert cyber attacks on UAV applications, it is necessary to deploy large-scale cooperative UAV defense by sharing trapped attack data in UAVs' honeypots.

B. Game Modeling for Honeypot-Based Defense

In the literature, various game-theoretical honeypot deception mechanisms have been proposed to enhance defense effectiveness. Garg *et al.* [10] investigate the honeypot deployment problem using a strategic game-theoretical deception model between attackers and the defender (i.e., the honeynet administrator) under imperfect information, where their Bayesian equilibrium strategies are analyzed. Tian *et al.* [15] study a honeypot defense game against APT attacks under industrial IoT, where the stable strategies of attackers and defenders are analytically derived under bounded rationality. Wang *et al.* [16] design a honeypot architecture to capture DDoS traffic on smart meters and devise a Bayesian game-theoretical model to model the interactions between DDoS attackers and defenders

in smart grids. La *et al.* [18] propose a Bayesian game-based deception model in honeypot networks containing an attacker and a defender, where the attacker can deceive the defender by exhibiting various behavior patterns ranging from suspicious to seemingly normal under incomplete information. Tian *et al.* [17] present a contract game model to motivate small-scale electricity suppliers (SESs) equipped with honeypots to contribute local defense data with power retailers to reduce system defense costs. Tsemogne *et al.* [19] design a two-player stochastic zero-sum game model to mitigate IoT botnet propagation to search for the optimal honeypot placement policy for the defender to deceive the attacker. Wahab *et al.* [20] propose a repeated Bayesian Stackelberg game model to detect smart attackers in the clouds, where the attack patterns are learned from risky VMs using honeypots by support vector machine (SVM) methods.

However, the above works are mainly built atop high-interaction honeypots on real hosts or VMs, which are inapplicable to UAV networks with high mobility and limited resources. In addition, UAVs' multi-dimensional private information, different levels of information asymmetry, and the defender's budget constraints are ignored in previous works on game-based honeypot defenses. Table I summarizes the key differences between our work and related research.

III. SYSTEM MODEL

This section introduces the system model, consisting of the network model, UAV mobility model, channel model, and threat model.

A. Network Model

Fig. 1 depicts a typical honeypot-based collaborative defense scenario in a UAV network, consisting of one GCS (denoted as G) and I flying UAVs. A group of UAVs (denoted as $\mathcal{I} = \{1, \cdots, I\}$) mounted with rich sensors are dispatched to a specific task area for immediate mission execution (e.g., power lines inspection). UAVs can exchange flying information for collision avoidance via air-to-air (A2A) links. Besides, each UAV is equipped with a low/medium-interaction honeypot system to allow emulation, recording, and analysis of its captured malicious activities to mitigate cyber attacks. Let S_i denote UAV i's private valid defense data (VDD) volume, which means the data size of unknown attack interaction logs gathered by the UAV honeypot [14]. UAVs are distinguished by their 2D private information: the marginal VDD cost and the communication delay. Let $\mathcal{J} = \{1, \cdots, J\}$ be the set of

UAV types. We refer to a UAV with $\theta_j \triangleq (C_j, T_j)$ as a type-j UAV. Here, C_j means the unit cost for VDD generation, VDD transmission, and privacy loss of type-j UAV. T_j is the communication delay of type-j UAV in transmitting VDD amount S_j (in bytes) to the GCS.

The GCS, as the coordinator of the UAV network, can communicate with UAVs via air-to-ground (A2G) links, perform UAV control (e.g., task assignment and trajectory planning), and carry out task data processing as well as security provisioning. Traditionally, the GCS obtains defense data through external security service providers. In our scenario, the GCS additionally obtains defense data from UAVs, which have deployed the honeypot, for quicker attack recognition and better situational awareness. To motivate UAVs' cooperation, the GCS offers a series of contracts $\Phi = \{T_{\max}, \{\Phi_j\}_{j \in \mathcal{J}}\}$ including the maximum communication delay $T_{\max}$ (for all UAV types) and J contract bundles $\{\Phi_j\}_{j \in \mathcal{J}} = \{S_j, R_j\}_{j \in \mathcal{J}}$ (one for each type). Here, S_j and R_j are the contributed VDD size and contractual reward (i.e., payment) of each type-j UAV, respectively. For any UAV fails to deliver its VDD within $T_{\max}$, the GCS offers a zero-payment contract. It is assumed that the type of each UAV remains unchanged in the entire honeypot defense process.

B. UAV Mobility Model

Based on [2], the total time horizon is evenly divided into T time slots with time length Δ_t. When Δ_t is sufficiently small, the instant location of UAV i in each time slot can be approximately fixed. According to the three-dimensional Cartesian coordinate system, UAV i's instant 3D location at t-th time slot is denoted as $\mathbf{l}_i(t) = [x_i(t), y_i(t), z_i(t)], \forall t \in \mathcal{T}, \forall i \in \mathcal{I}$. Here, $[x_i(t), y_i(t)]$ is the instantaneous horizontal coordinate of UAV i at time slot t. For each UAV i, its hover height $z_i(t)$ is fixed during executing each mission to ensure continuous flight and avoid frequent ascent/descent for minimized energy consumption [23]. The trajectories of UAVs are predetermined and controlled by the GCS G, which satisfies:

$$
\begin{cases}
\mathbf{l}_i = \{\mathbf{l}_i(1), \cdots, \mathbf{l}_i(t), \cdots, \mathbf{l}_i(T)\}, & (1) \\
\mathbf{l}_i(t+1) = V_i(t) \cdot \mathbf{w}_i(t) + \mathbf{l}_i(t), 1 \leq t \leq T-1, & (2) \\
\text{s.t. } ||\mathbf{l}_i(t+1) - \mathbf{l}_i(t)|| \leq \Delta_t V_{\max}^i. & (3)
\end{cases}
$$

In Eq. (1), $\mathbf{l}_i(1)$ and $\mathbf{l}_i(T)$ are the preset starting and ending locations of UAV i in the working area, respectively. In Eq. (2), $V_i(t)$ and $\mathbf{w}_i(t)$ are the flying velocity and trajectory direction of UAV i at t-th time slot, respectively. In Eq. (3), $V_{\max}^i$ is UAV i's maximum velocity.

C. Channel Model

1) A2A Channel Model. The A2A channel path loss (in dB) between UAVs i and k can be regarded as LoS-dominant and distance-dependent [24], i.e., $\Upsilon_{i,k}^{\mathrm{A2A}}(t) = (d_{i,k}(t))^{-\iota}$, where ι means the path loss exponent and $d_{i,k}(t)$ is the 3D Euclidean distance between two UAVs i and k. Let B^{A2A} denote the

A2A channel bandwidth. At time slot t, based on the Shannon bound, the available data rate from UAV i to UAV k is

$$
\gamma_{i,k}(t) = B^{\mathrm{A2A}} \log_2 \left(1 + \frac{P_i^{\mathrm{Tr}}(t) \Upsilon_{i,k}^{\mathrm{A2A}}(t)}{\sum_{l \in \mathcal{I}, l \neq i} P_l^{\mathrm{Tr}}(t) \Upsilon_{l,k}^{\mathrm{A2A}}(t) + \varphi^2} \right),
\tag{4}
$$

where $P_i^{\mathrm{Tr}}(t)$ is UAV i's transmit power at time slot t. $\sum_{l \in \mathcal{I}, l \neq i} P_l^{\mathrm{Tr}}(t) \Upsilon_{l,k}^{\mathrm{A2A}}(t)$ represents the sum of interferences from other UAVs to UAV k at time slot t. φ^2 is the power of the additive white Gaussian noise.

2) A2G Channel Model. For the A2G/G2A communications, the average pathloss (in dB) between UAV i and GCS follows the large-scale channel fading model depending on the occurrence chances of LoS and non-LoS (NLoS) links [25], i.e.,

$$
\Upsilon_{i,G}^{\mathrm{A2G}}(t) = 20 \log \left(4\pi d_{i,G} \phi_c / c \right) + \mathrm{Pr}_{\mathrm{LoS}}(t) \kappa_{\mathrm{LoS}} \\
+ \mathrm{Pr}_{\mathrm{NLoS}}(t) \kappa_{\mathrm{NLoS}},
\tag{5}
$$

where κ_{LoS} and κ_{NLoS} are additional attenuation factors of free space pathloss for LoS and NLoS links, respectively. ϕ_c is the carrier frequency, c means the speed of light, and $d_{i,G}$ is the horizontal distance between UAV i and the GCS. The LoS probability $\mathrm{Pr}_{\mathrm{LoS}}(t)$ is a modified logistic function of the elevation angle $\theta_{i,G}(t) = \arctan(\frac{z_i(t) - h_G}{d_{i,G}})$ [25], i.e.,

$$
\mathrm{Pr}_{\mathrm{LoS}}(t) = [1 + \iota_1 \exp(-\iota_2(\theta_{i,G}(t) - \iota_1))]^{-1}.
\tag{6}
$$

Here, ι_1 and ι_2 are environment-related variables, h_G is the height of GCS, and $\mathrm{Pr}_{\mathrm{NLoS}}(t) = 1 - \mathrm{Pr}_{\mathrm{LoS}}(t)$.

For A2G/G2A data transmissions, based on works [25], [26], it is assumed that each UAV is allocated a dedicated sub-channel with orthogonal resource blocks for uplink transmission, thereby there exists no mutual interference between UAVs. Let B^{A2G} denote the uplink A2G channel bandwidth. At time slot t, the available uplink data rate from UAV i to the GCS is

$$
\gamma_{i,G}(t) = B^{\mathrm{A2G}} \log_2 \left(1 + \frac{P_i^{\mathrm{A2G}} 10^{-\Upsilon_{i,G}^{\mathrm{A2G}}(t)/10}}{\varphi^2} \right).
\tag{7}
$$

D. Threat Model

In the cooperative UAV defense services based on honeypot data sharing, the following two threats that may deteriorate system efficiency and defense performance are considered.

- **Selfish UAVs:** UAV participation is the key to the success of collaborative UAV defense services. However, as the deployment of honeypots and VDD data transmission operations can consume additional battery power of resource-limited UAVs, UAV owners (as rational and selfish individuals) may be reluctant to participate in the joint defense process [27]. Thereby, the overall defense performance can be reduced as it lacks enough participants.
- **Free-riding UAVs:** Self-interested UAVs may launch free-riding attacks to gain an unfair advantage without contributing to the joint defense process, thereby inhibiting the enthusiasm and willingness of other honest UAVs [28]. For example, free-riding UAVs may enjoy joint defense services by sharing redundant and outdated honeypot data to cheat more rewards.

IV. HONEYPOT GAME THEORETICAL COOPERATIVE DEFENSE FRAMEWORK

In this section, we first formulate the UAV honeypot game for active cooperative defense among UAVs. Then, we define the equilibrium and design goals of the UAV honeypot game.

A. UAV Honeypot Game Formulation

Definition 1 (UAV Honeypot Game): During honeypot data sharing process, the interactions between UAVs and the GCS can be formulated as a honeypot game $\mathcal{G} = \{\{\mathcal{J}, G\}, \{T_{\max}, \{S_j, R_j\}_{j \in \mathcal{J}}\}, \{\{\mathcal{U}_j\}_{j \in \mathcal{J}}, \mathcal{U}_G\}\}$, which includes the following main components:

- *Players.* The players in game $\mathcal{G}$ are (i) UAVs with diverse VDD-delay types in $\mathcal{J}$ and (ii) the GCS G.
- *Strategies.* The strategy of the GCS is to determine the maximum communication latency $T_{\max}$ and design a set of feasible VDD-reward contracts $\{S_j, R_j\}_{j \in \mathcal{J}}$ to optimize its overall payoff. The strategy of each UAV is to select an optimal contract item for maximized payoff.
- *Payoffs.* The payoffs (or utilities) of each type-j UAV and the GCS are denoted as $\mathcal{U}_j$ and $\mathcal{U}_G$, respectively.

Utility of UAV. The utility of type-j UAV that chooses the contract item $\Phi_j = \{S_j, R_j\}$ is the revenue minuses its cost:

$$\mathcal{U}_j(\Phi_j) = \begin{cases} R_j - C_j^1 S_j - C_j^2 S_j - C_0, & \text{if } T_j \leq T_{\max}; \\ -C_j^1 S_j - C_j^2 S_j - C_0, & \text{if } T_j > T_{\max}. \end{cases} \quad (8)$$

In (8), C_j^1 is the unit cost of VDD creation and transmission, which is related to UAV's honeypot and communication capabilities. C_j^2 is UAV i's unit privacy cost of VDD sharing. Both C_j^1 and C_j^2 are UAV's private information. Here, $C_j = C_j^1 + C_j^2$. C_0 is UAV's honeypot deployment cost.

To improve communication efficiency, an *A2A/A2G mode selection method* is designed. Specifically, if UAV j experiences a high signal-to-noise ratio (SNR) for the A2G link, it directly uploads its encrypted VDD via A2G mode. Otherwise, it alternatively delivers data to a neighboring UAV j' operating in A2G mode and relays to the GCS. Let $\alpha_j = \{0, 1\}$ be a binary variable, where $\alpha_j = 1$ means it works on A2G mode, otherwise $\alpha_j = 0$. We have

$$T_j = \alpha_j \times \frac{S_j}{\gamma_{j,G}} + (1 - \alpha_j) \times \left(\frac{S_j}{\gamma_{j,j'}} + \frac{S_j}{\gamma_{j',G}} \right), \quad (9)$$

where $\gamma_{j,G}$ and $\gamma_{j',G}$ are data rates between UAV j/j' and GCS G according to Eq. (7). $\gamma_{j,j'}$ is the data rate between UAVs j and j' according to Eq. (4).

Utility of GCS. The utility of the GCS is the overall satisfaction of cooperative defense minuses its total payments:

$$\mathcal{U}_G(\Phi) = \sum_{j \in \mathcal{J}} \varpi \frac{N_j}{T_j} \log \left(1 + \mathbb{1}_{T_j \leq T_{\max}} S_j \right) - \mathbb{1}_{T_j \leq T_{\max}} N_j R_j. \quad (10)$$

In (10), the first term indicates the satisfaction related to UAV's VDD size and communication latency. Based on [5], [29], we utilize the natural logarithmic function for satisfaction modelling. ϖ is a positive satisfaction factor. N_j is the number of type-j UAVs, which satisfies $\sum_{j \in \mathcal{J}} N_j = I$. $\mathbb{1}_{T_j \leq T_{\max}}$ is

an indicator function, whose value equals to one if $T_j \leq T_{\max}$ holds; otherwise its value is zero.

Social Surplus. The social surplus of the UAV honeypot game is defined as the sum of the utilities of the GCS and all participating UAVs in collaborative honeypot defense, i.e.,

$$\mathcal{S}(\Phi) = \mathcal{U}_G(\Phi) + \sum_{j \in \mathcal{J}} \mathbb{1}_{T_j \leq T_{\max}} \mathcal{U}_j(\Phi_j) \quad (11)$$

$$= \sum_{j \in \mathcal{J}} \varpi \frac{N_j}{T_j} \log \left(1 + \mathbb{1}_{T_j \leq T_{\max}} S_j \right) - \mathbb{1}_{T_j \leq T_{\max}} N_j \left(C_j S_j - C_0 \right).$$

B. Equilibrium and Design Goals of UAV Honeypot Game

The equilibrium strategy of the game $\mathcal{G}$ (i.e., the solution of the game) is to design the *optimal contracts* for all types of UAVs, namely, $\Phi^* = \{T_{\max}, \{S_j^*, R_j^*\}_{j \in \mathcal{J}}\}$, while enforcing *budget feasibility*, *contractual feasibility*, and *contractual fairness*. Budget feasibility (BF) means that the GCS could only afford a constrained system budget (i.e., limited overall rewards) in each defense process in the honeypot game.

Definition 2 (Budget Feasibility (BF)): A contract is budget feasible, if the total reward for all participating UAVs does not exceed the overall budget Ω, i.e.,

$$\mathbb{1}_{T_j \leq T_{\max}} N_j R_j \leq \Omega. \quad (12)$$

Apart from BF, contractual feasibility and optimality are basic goals of contract mechanism design, which are formally defined as follows.

Definition 3 (Contractual Feasibility): A contract is feasible if each type of UAV has the greatest and non-negative utility when faithfully adopting the contract item designed for its type.

Definition 4 (Contractual Optimality): Among all feasible contracts, a contract is optimal if it maximizes the utility of the contract designer (i.e., the GCS).

According to the revelation principle [30], a contract satisfying the contractual feasibility is equivalent to that the individual rationality (IR) and incentive compatibility (IC) constraints are satisfied simultaneously for all types of UAVs. The IR and IC constraints are formally defined as follows:

Definition 5 (Individual Rationality (IR)): If and only if each type-j UAV can obtain non-negative utility when faithfully adopting the contract item $\Phi_j = (S_j, R_j)$ designed for its type, then the contract satisfies IR constraint. Mathematically,

$$\mathcal{U}_j(\Phi_j) \geq 0, \forall j \in \mathcal{J}. \quad (13)$$

Definition 6 (Incentive Compatibility (IC)): If and only if each type-j UAV prefers to faithfully adopt the contract item $\Phi_j = (S_j, R_j)$ designed for its type rather than other contract items, then the contract satisfies IR constraint. Mathematically,

$$\mathcal{U}_j(\Phi_j) \geq \mathcal{U}_j(\Phi_{j'}), \forall j, j' \in \mathcal{J}, j \neq j'. \quad (14)$$

In addition to optimality, fairness is another desirable target of contract mechanism design. Based on the literature [31], the definitions of participation fairness and reward fairness are first introduced. Then, the contractual fairness is defined based on these two aspects.

Definition 7 (Participation Fairness): Participation fairness is satisfied if any rational and selfish UAV honestly follows the contractual procedure. Namely, they have no incentive to withdraw from the collaborative honeypot data sharing process and report false individual types to demand more compensation.

Definition 8 (Reward Fairness): If 1) higher rewards are given to participating UAVs that contribute more VDD in collaborative defense, and 2) no rewards are given to non-participating UAVs, then reward fairness is satisfied.

Definition 9 (Contractual Fairness): If both participation fairness and reward fairness are satisfied, then the contract is said to be fair.

In this paper, we design the optimal contracts for UAVs to solve the honeypot game under the following three levels of information asymmetry.

- *Complete information scenario (benchmark).* In this ideal situation, there exists no information asymmetry and the GCS knows the private type information of each UAV.
- *Partial information asymmetry scenario.* The GCS has prior knowledge of the distribution of UAV types (i.e., $N_j/I, \forall j \in \mathcal{J}$) and the total number of UAVs (i.e., I), but is unaware of which UAV belongs to which type. Note that the distribution of UAV types can be obtained in various manners, e.g., making a survey questionnaire.
- *Complete information asymmetry scenario.* The GCS only knows the total number of UAVs and the total number of UAV types.

V. OPTIMAL CONTRACT DESIGN IN COMPLETE INFORMATION

In the complete information scenario, the contract designer (i.e., the GCS) knows the private type of each UAV. Thereby, it can check whether UAVs faithfully adopt the contract items designed for their types. Correspondingly, the GCS only needs to ensure that all types of UAVs can obtain non-negative utility in the honeypot game. Therefore, the contract feasibility constraint is equivalent to the IR constraint.

A. Optimization Problem in Complete Information

Problem 1 (GCS's optimization problem under complete information scenario):

$$\max_{\Phi} \mathcal{U}_G(\Phi)$$
$$\text{s.t.} \begin{cases} 0 \leq S_j \leq S_{\max}, \forall j \in \mathcal{J}, \\ \text{BF constraint (12)}, \forall j \in \mathcal{J}, \\ \text{IR constraint (13)}, \forall j \in \mathcal{J}. \end{cases} \quad (15)$$

Remark. The first constraint means that the amount of VDD contributed by each type of UAV is constrained by the upper bound $S_{\max}$ and the lower bound 0. The second one is the BF constraint, and the third one is the IR constraint.

B. Optimal Contract in Complete Information

Next, we solve Problem 1 in two steps. First, for any given VDD size, Lemma 1 gives the optimal reward policy for the GCS. Second, by substituting the optimal reward strategy into

the GCS's utility function, Theorem 1 proves the optimal contract VDD size strategy. To simplify the expression, let $\mathcal{J}'$ be the set of UAV types that satisfy $\mathbb{1}_{T_j \leq T_{\max}} = 1$, i.e., $\mathcal{J}' = \{j | T_j \leq T_{\max}\}$. Then we reindex UAV types in $\mathcal{J}'$ in descending order of the marginal VDD cost, i.e., $C_1 > C_2 > \cdots > C_{J'}$, where $J' = |\mathcal{J}'|$.

Lemma 1: For any VDD data size $S_j \in [0, S_{\max}]$, the optimal reward strategy for the GCS is:

$$R_j^*(S_j) = \begin{cases} 0, & \forall j \notin \mathcal{J}'; \\ C_j S_j + C_0, & \forall j \in \mathcal{J}'. \end{cases} \quad (16)$$

Proof: Please refer to Appendix A. ∎

Lemma 2: The BF constraint in (12) can be simplified as:

$$\sum\nolimits_{j=1}^{J'} N_j R_j = \Omega. \quad (17)$$

Proof: Please refer to Appendix B. ∎

Remark. Lemmas 1 and 2 mean that, under the complete information scenario, for non-participating UAVs, the GCS will provide a zero-payment contract; for participating UAVs, the GCS will design optimal contract items by exhausting the available budget such that all participating UAVs will receive zero utility.

For any participating UAV ($\forall j \in \mathcal{J}'$), by substituting $R_j^* = C_j S_j + C_0$ into $\mathcal{U}_G(\Phi)$ in (10), the utility function of the GCS can be rewritten as a function of S_j:

$$\mathcal{U}_G(S_j) = \sum\nolimits_{j \in \mathcal{J}'} \frac{\varpi N_j}{T_j} \log(1 + S_j) - N_j(C_j S_j + C_0). \quad (18)$$

Based on Lemmas 1 and 2, the optimization problem (15) can be equivalently formulated as below.

Problem 1-1 (Simplified Problem 1 with reduced BF and IR constraints):

$$\max_{\Phi} \mathcal{U}_G(S_j)$$
$$\text{s.t.} \begin{cases} 0 \leq S_j \leq S_{\max}, \forall j \in \mathcal{J}', \\ \sum_{j \in \mathcal{J}'} N_j R_j = \Omega, \\ R_j = C_j S_j + C_0, \forall j \in \mathcal{J}'. \end{cases} \quad (19)$$

The above Problem 1-1 can be solved via Lagrange analysis with KKT conditions, where its Lagrangian function is:

$$\mathcal{L}(S_j, \lambda_1) = \mathcal{U}_G(S_j) + \lambda_1 \Big(\sum\nolimits_{j=1}^{J'} N_j(C_j S_j + C_0) - \Omega \Big)$$
$$= \sum_{j=1}^{J'} \left[\frac{\varpi N_j}{T_j} \log(1 + S_j) + (\lambda_1 - 1) N_j(C_j S_j + C_0) \right] - \lambda_1 \Omega, \quad (20)$$

where λ_1 denotes the Lagrange multiplier.

The following Theorem 1 further deduces the optimal contractual VDD size for each type of UAV.

Theorem 1: Under the complete information scenario, the VDD size and contract reward in the optimal contract are:

1) $\forall j \notin \mathcal{J}', S_j = R_j = 0$.
2) $\forall j \in \mathcal{J}'$,

$$\begin{cases} S_j^* = \min\left\{ S_{\max}, \max\left\{ \frac{\Lambda}{T_j C_j} - 1, 0 \right\} \right\}, & (21) \\ R_j^* = C_j S_j^* + C_0, & (22) \end{cases}$$

where

$$\Lambda = \frac{\Omega + \sum_{j=1}^{J'} N_j C_j - C_0 \sum_{j=1}^{J'} N_j}{\sum_{j=1}^{J'} \frac{N_j}{T_j}}. \quad (23)$$

Proof: Please refer to Appendix C. ∎

Corollary 1: From the (18), it can be deduced that in the complete information scenario, the GCS's optimal utility is equivalent to the optimal social surplus. Therefore, the optimal contract under the complete information scenario derived in Theorem 1 is also a social optimal contract strategy.

VI. OPTIMAL CONTRACT DESIGN IN PARTIAL INFORMATION ASYMMETRY

Unlike the complete information scenario, there usually exists information asymmetry between the GCS and UAVs in practical applications, where the optimization problem under incomplete information scenarios is formulated as below. In the partial information asymmetry scenario, the GCS only knows the total number of UAVs (i.e. I) and the private type distribution of UAVs (i.e. $p_j = \{\frac{N_j}{I}\}_{\forall j \in \mathcal{J}}$).

A. Optimization Problem in Incomplete Information

Problem 2 (GCS's optimization problem under incomplete information scenario):

$$\max_{\Phi} \mathcal{U}_G(\Phi)$$

$$\text{s.t.} \begin{cases} 0 \le S_j \le S_{\max}, \forall j \in \mathcal{J}, \\ \text{BF constraint (12)}, \forall j \in \mathcal{J}, \\ \text{IR constraint (13)}, \forall j \in \mathcal{J}, \\ \text{IC constraint (14)}, \forall j \in \mathcal{J}. \end{cases} \quad (24)$$

Remark. The first three constraints are the same as Problem 1, and the fourth constraint is the IC constraint in (14). Constraints (13) and (14) enforce the contractual feasibility.

Notably, there are J^2 IR and IC constraints in (13) and (14) in Problem 2, making it difficult to resolve Problem 2, particularly when J is large. In what follows, IR and IC constraints are first transformed with reduced numbers using Lemma 3 and Theorem 2. Then, given an arbitrary monotonic VDD size sequence $\mathbf{S}$, Theorem 3 gives the optimal reward policy $\mathbf{R}^*(\mathbf{S})$. Then, based on these two theorems, Problem 2 is transformed into the equivalent Problem 2-1 with reduced constraints, and Theorem 4 derives the optimal VDD size sequence $\widetilde{\mathbf{S}}^*$ for the relaxed form of the problem without the monotonicity constraint. Lastly, according to the rationale in Theorem 5, an optimal dynamic allocation algorithm is designed in Algorithm 1 to acquire the optimal VDD size strategy $\mathbf{S}^*$ and the optimal reward strategy $\mathbf{R}^*(\mathbf{S}^*)$ under budget constraints.

B. Optimal Contract in Partial Information Asymmetry

Lemma 3: If IC constraints in (14) hold for all UAV types, then IR constraints in (13) can be replaced by $\mathcal{U}_1(\Phi_1) \ge 0$.

Proof: As the IC constraint is satisfied for all UAV types, we have

$$R_j - C_j S_j - C_0 \ge R_1 - C_j S_1 - C_0 \ge R_1 - C_1 S_1 - C_0. \quad (25)$$

Lemma 3 implies that if type-1 UAV satisfies the IR constraint, then all types of UAVs satisfy the IR constraint. We further characterize the feasibility of the contract in the following Theorem 2.

Theorem 2: A contract $\Phi = \{T_{\max}, \{\Phi_j\}_{j \in \mathcal{J}}\}$ is feasible if and only if the following conditions are met:

1) $\forall j \notin \mathcal{J}', S_j = R_j = 0$.
2) $\forall j \in \mathcal{J}'$,

$$\begin{cases} 0 \le S_1 \le \cdots \le S_{J'} \& 0 \le R_1 \le \cdots \le R_{J'}, & (26) \\ R_1 - C_1 S_1 - C_0 \ge 0, & (27) \\ C_j(S_j - S_{j-1}) \le R_j - R_{j-1} & \\ \qquad \le C_{j-1}(S_j - S_{j-1}), \ j = 2, \cdots, J'. & (28) \end{cases}$$

Proof: Please refer to Appendix D. ∎

Remark. For any UAV type $j \notin \mathcal{J}'$, Theorem 2 shows that the required contractual VDD size and reward are zero. For the case $j \in \mathcal{J}'$, constraints (26) and (28) correspond to IC constraints, while constraint (27) corresponds to IR constraints. Constraint (26) means that the GCS should demand more VDD from UAVs with smaller marginal costs and offer more rewards to them. Constraint (27) indicates that if the UAV with the highest marginal cost satisfies the IR constraint, then all types of UAVs meet IR constraints. Constraint (28) implies that if type-j and type-$(j-1)$ UAVs satisfy the IC constraint, then type-j UAV and any other type of UAV also satisfy the IC constraint.

Corollary 2: For any feasible contract $\{S_j, R_j\}_{j \in \mathcal{J}'}$, the utilities of different types of UAVs satisfy:

$$\mathcal{U}_1(\Phi_1) < \cdots < \mathcal{U}_j(\Phi_j) < \cdots < \mathcal{U}_{J'}(\Phi_{J'}), \forall j \in \mathcal{J}'. \quad (29)$$

Proof: According to Theorem 2, the UAV that requires more rewards should provide more VDD data, namely, $R_j \ge R_k$ and $S_j \ge S_k$ meet simultaneously. If $C_j < C_k$, we have

$$\begin{aligned} \mathcal{U}_j(\Phi_j) &= R_j - C_j S_j - C_0 \\ &\ge R_k - C_j S_k - C_0 \quad \text{(IC)} \\ &> R_k - C_k S_k - C_0 = \mathcal{U}_k(\Phi_k). \quad (30) \end{aligned}$$

It can be concluded that when $C_k > C_j$, we have $\mathcal{U}_k(\Phi_k) < \mathcal{U}_j(\Phi_j)$. Since $C_1 > C_2 > \cdots > C_{J'}$, we have $\mathcal{U}_1(\Phi_1) < \cdots < \mathcal{U}_j(\Phi_j) < \cdots < \mathcal{U}_{J'}(\Phi_{J'})$, $\forall j \in \mathcal{J}'$. ∎

In the following Theorem 3, we derive the optimal reward strategy $\mathbf{R}^*(\mathbf{S})$.

Theorem 3: Given any VDD size sequence $\mathbf{S} = \{S_j\}_{j \in \mathcal{J}'}$ meeting $0 \le S_1 \le \cdots \le S_{J'} \le S_{\max}$, the unique optimal reward strategy $\mathbf{R}^* = \{R_j^*\}_{j \in \mathcal{J}'}$ is attained by:

1) $\forall j \notin \mathcal{J}', R_j^*(\mathbf{S}) = 0$.
2) $\forall j \in \mathcal{J}'$, we have

$$R_j^*(\mathbf{S}) = \begin{cases} C_j S_j + C_0, & j = 1; \\ R_{j-1}^*(\mathbf{S}) + C_j(S_j - S_{j-1}), & \\ & j = 2, ..., J'. \end{cases} \quad (31)$$

Proof: Please refer to Appendix E. ∎

Remark. Theorem 3 shows that the optimal reward positively correlates with UAV's shared VDD size, ensuring contractual fairness. The BF constraint in (12) can be simplified as $\sum_{j=1}^{J'} N_j R_j = \Omega$. The proof is similar to that of Lemma 2.

According to Theorems 2–3, the original Problem 2 can be rewritten into the following simplified form.

Problem *2-1 (Simplified Problem 2 with reduced BF, IR, and IC constraints):*

$$\max_{\Phi} \mathcal{U}_G(\Phi)$$

$$\text{s.t.} \begin{cases} \text{C1}: 0 \leq S_1 \leq \cdots \leq S_{J'} \leq S_{\max}, \\ \text{C2}: R_1 - C_1 S_1 - C_0 = 0, \\ \text{C3}: R_j - C_j S_j = R_{j-1} - C_j S_{j-1}, \forall j = 2, \cdots, J', \\ \text{C4}: \sum_{j \in \mathcal{J}} N_j R_j = \Omega, \end{cases} \quad (32)$$

Besides, $\forall j \in \mathcal{J}'$, the optimal reward strategy in (31) can be reformulated by iteration as follows:

$$R_j^*(\mathbf{S}) = \begin{cases} C_j S_j + \sum_{k=1}^{j-1}(C_k - C_{k+1}) S_k + C_0, \\ \qquad\qquad\qquad\qquad j = 2, \cdots, J'; \\ C_j S_j + C_0, \qquad j = 1. \end{cases} \quad (33)$$

Theorem *4:* Under partial information asymmetry, the solution of the Problem 2-1 without constraint C1 is the optimal contractual VDD size strategy, i.e.,

$$S_j^* = \min\left\{ S_{\max}, \max\left\{ \frac{N_j}{A_j T_j} \cdot \mathfrak{R} - 1, 0 \right\} \right\}, \quad (34)$$

where $\mathfrak{R}$, A_j, and ΔC_j are defined as follows:

$$\mathfrak{R} = \frac{\Omega + \sum_{j=1}^{J'} A_j - C_0 \sum_{j=1}^{J'} N_j}{\sum_{j=1}^{J'} \frac{N_j}{T_j}}. \quad (35)$$

$$A_j = \begin{cases} N_{J'} C_{J'}, & j = J'; \\ N_j C_j + \Delta C_j \sum_{k=j+1}^{J'} N_k, & j \leq J' - 1. \end{cases} \quad (36)$$

$$\Delta C_j = C_j - C_{j+1}. \quad (37)$$

Proof: Please refer to Appendix F. ∎

Remark. If $\mathbf{S}^* = \{S_j^*\}_{j \in \mathcal{J}'}$ is an non-decreasing sequence (i.e., C1 holds), $\mathbf{S}^*$ is the solution of Problem 2-1. Nevertheless, the monotonicity constraint C1 may not hold in general UAV type distributions. Based on [29], a dynamic VDD size assignment method is designed to cope with this issue through bunching and ironing.

Theorem *5:* Define $\tilde{y}_n^* = \arg\max_{y_n} \Gamma_n(y_n)$ and $\Gamma_n(y)$ as a convex function of y, $\forall n = 1, \cdots, N$. If $\tilde{y}_N^* \geq \tilde{y}_2^* \geq \cdots \geq \tilde{y}_1^*$ holds, we have $y_1^* = y_2^* = \cdots = y_N^*$, where

$$\{y_n^*\} = \arg\max_{\{y_n\}} \sum_{n=1}^{N} \Gamma_n(y_n), \forall n = 1, \cdots, N$$
$$\text{s.t. } y_1 \geq y_2 \geq \cdots \geq y_N. \quad (38)$$

Proof: The detailed proof can refer to [29]. As a single-variable optimization problem, the problem in (38) can be efficiently solved by methods such as binary search. ∎

In Algorithm 1, a dynamically optimal VDD sequence allocation method with low-complexity is designed in lines 11-13 to iteratively search for sub-sequences that violate contractual feasibility and adjust them by Theorem 5. The maximum number of iterations is $J' - 1$. Specifically, for any decreasing sub-sequence $\{S_m^*, S_{m+1}^*, \cdots, S_n^*\} \subseteq \mathbf{S}^*$, all its

---

Algorithm 1: Budget-Constrained Optimal Contract Assignment in Partial Information Asymmetry

1 **Input:** $\mathcal{J}'$, N_j, θ_j, ϖ, $S_{\max}$, C_0, $T_{\max}$;
2 **Output:** Optimal contract $\hat{\Phi}^* = \{\{\hat{S}_j^*, \hat{R}_j^*\}_{j \in \mathcal{J}}\}$;
3 **for** $j \in \mathcal{J} \backslash \mathcal{J}'$ **do**
4   Set $S_j^* = R_j^* = 0$;
5 **for** $j \in \mathcal{J}'$ **do**
6   Calculate the relaxed optimal contract VDD size strategy $\widetilde{S}_j^*$ via Theorem 4;
7   **if** $\widetilde{S}_j^* > S_{\max}$ **then**
8   Set $\widetilde{S}_j^* = S_{\max}$;
9   **else if** $\widetilde{S}_j^* < 0$ **then**
10   Set $\widetilde{S}_j^* = 0$;

11 **while** *VDD sequence* $\{\widetilde{S}_j^*\}_{j \in \mathcal{J}'}$ *does not satisfy the contract feasibility* **do**
12   Search for one of the subsequences $\{\widetilde{S}_l^*, \widetilde{S}_{l+1}^*, \cdots, \widetilde{S}_m^*\} \subseteq \{\widetilde{S}_j^*\}_{j \in \mathcal{J}'}$;
13   Dynamically adjust the infeasible subsequence by (39);
14 **for** $j \in \mathcal{J}'$ **do**
15   Compute the optimal contract reward strategy $R_j^* = R_j^*(\mathbf{S}^*)$ by (33);

---

elements are dynamically adjusted by resolving the following single variable optimization problem:

$$S_l^* = \arg\max_{S_l} \sum_{l=m}^{n} \Im(S_l), \forall l = m, m+1, \cdots, n. \quad (39)$$

Remark. The above process in (39) is repeated until all the sub-sequences in $\mathbf{S}^*$ obtained from (68)–(37) are non-decreasing. After that, the optimal contracts $\Phi^* = \{T_{\max}, \{S_j^*, R_j^*\}_{j \in \mathcal{J}}\}$ can be designed for all types of UAVs.

Algorithm 1 describes the optimal contract design process in the UAV honeypot game under partial information asymmetry and budget limits. First, in lines 3–4, the GCS sets up a zero-payment contract for non-participating UAVs and UAVs that cannot transmit VDD in time. Next, in lines 5–10, for UAVs involved in honeypot defense, the GCS calculates the optimal contract VDD size strategy $\widetilde{S}_j^*$ according to (68)–(37). Lines 11–13 represent the dynamic allocation process of the optimal VDD size sequence. After obtaining the optimal VDD size sequence $\mathbf{S}^*$, in lines 14–15, the GCS calculates the optimal contract reward R_j^* by (33). In each round of collaborative defense based on honeypot game, each participating UAV uploads its VDD data according to the contract data size and receives the corresponding contract reward from the GCS after completing data transmission in time.

Theorem *6:* The optimal contracts derived in Algorithm 1 satisfy contractual fairness.

Proof: According to Theorem 3, any UAV that does not participate in honeypot data sharing will receive a non-positive payoff. Since the optimal contracts satisfy IR constraints, the payoff of an honest UAV is always non-negative and no less than the case when it does not participate. Hence, the designed optimal contract satisfies participation fairness. According to Theorem 3, for every type-j UAV, its optimal contract reward $R_j^*(\mathbf{S}^*)$ increases with the increase of the contract VDD size S_j^*. Furthermore, for non-participating UAVs, the proposed

contract mechanism enforces a zero-payment strategy. Hence, the optimal contracts guarantee reward fairness. According to Definition 8, the obtained optimal contracts in Algorithm 1 satisfy contractual fairness. ∎

VII. OPTIMAL DYNAMIC CONTRACT DESIGN IN COMPLETE INFORMATION ASYMMETRY

In this section, we design the optimal dynamic contract in complete information asymmetry. Different from the partial information asymmetry scenario, the GCS has no prior knowledge of the UAVs' private types under the complete information asymmetry. Thereby, both the GCS and UAVs can apply policy hill-climbing (PHC) learning, a model-free RL technique, to make optimal reward and VDD size strategies in dynamic contract design through trials, without explicitly knowing UAVs' private parameters (e.g., UAV type distribution). For both sides, the strategy-making process can be modelled as a finite Markov decision process (MDP).

A. PHC-based Reward Strategy of GCS

At each time slot t, the system state vector $\mathbf{W}^t = (W_1^t, \cdots, W_{J'}^t)$ observed by the GCS consists of the previous VDD size of each type of UAV, i.e., $\mathbf{W}^t = \mathbf{S}^{t-1}$. For simplicity, the GCS uniformly quantizes the reward strategy into $A+1$ levels, i.e., $R_j \in \mathcal{A} = \{\frac{a}{A} \cdot R_{\max}\}_{0 \le a \le A}$, where $R_{\max}$ is the maximum reward that the GCS pays to a UAV. Let $\mathcal{Q}(\mathbf{W}^t, \mathbf{R}^t)$ represent the GCS's Q-function (i.e., expected long-term discounted utility) of each state-action pair, which is updated based on the iterative Bellman equation:

$$\mathcal{Q}\left(W_j^t, R_j^t\right) \leftarrow (1-\kappa_1)\mathcal{Q}\left(W_j^t, R_j^t\right) + \kappa_1 \left\{\mathcal{U}_G\left(W_j^t, R_j^t\right) \right.$$
$$\left. + \varphi_1 \max_{R_j} \mathcal{Q}\left(W_j^{t+1}, R_j^{t+1}\right)\right\}, \forall j \in \mathcal{J}', \quad (40)$$

where κ_1 is the learning rate, and φ_1 is the discount factor. W_j^{t+1} is the new state of type-j UAV at time slot $t+1$, which is transferred from state W_j^t with action R_j^t.

To tradeoff the exploration and exploitation in PHC, the mixed-strategy table $\pi(\mathbf{W}^t, \mathbf{R}^t)$ is updated by increasing the chance of behaving greedily by a small value ρ_1, and lowering other chances by $-\frac{\rho_1}{A+1}$, i.e.,

$$\pi\left(W_j^t, R_j^t\right) \leftarrow \pi\left(W_j^t, R_j^t\right)$$
$$+ \begin{cases} \rho_1, & \text{if } R_j^t = \arg\max_{R_j} \mathcal{Q}\left(W_j^t, R_j\right); \\ -\frac{\rho_1}{A+1}, & \text{otherwise.} \end{cases} \quad (41)$$

The GCS opts its contractual reward strategy $R_j^t, \forall j \in \mathcal{J}'$ based on the above mixed-strategy table, i.e.,

$$\Pr\left(R_j^t = \hat{R}_j\right) = \pi\left(W_j^t, \hat{R}_j\right), \forall \hat{R}_j \in \mathcal{A}. \quad (42)$$

The hotbooting PHC-based optimal contractual reward strategy-making process of the GCS is summarized in lines 4–10 in Algorithm 2.

Algorithm 2: Optimal Dynamic Contract with Hotbooting PHC in Complete Information Asymmetry

1 **Initialize:** κ_1, κ_2, φ_1, φ_2, ρ_1, ρ_2, $\mathbf{W}^0$, $\tilde{W}_j^0$, A, B;
2 Perform hotbooting process and obtain $\mathcal{Q} = \mathcal{Q}_p$, $\pi = \pi_p$, $\tilde{\mathcal{Q}} = \tilde{\mathcal{Q}}_p$, $\tilde{\pi} = \tilde{\pi}_p$;
3 **for** $t = 1, 2, \cdots, T_e$ **do**
4   **Layer 1: Hotbooting PHC-Based Reward Strategy of the GCS;**
5   Set system state $\mathbf{W}^t = \mathbf{S}^{t-1}$;
6   Select reward action $\mathbf{R}_j^t$ by (42);
7   Observe and evaluate the VDD size $\mathbf{S}^t$;
8   Evaluate reward $\mathcal{U}_G\left(W_j^t, R_j^t\right)$ by (10);
9   Update $\mathcal{Q}\left(W_j^t, R_j^t\right)$ by (40);
10   Update $\pi\left(W_j^t, R_j^t\right)$ by (41);
11   **Layer 2: Hotbooting PHC-Based VDD Size Strategy of Each Type of UAV;**
12   Set system state $\tilde{W}_j^t = R_j^{t-1}$;
13   Select VDD size action S_j^t by (45);
14   Observe the reward R_j^t;
15   Evaluate reward $\mathcal{U}_j\left(\tilde{W}_j^t, S_j^t\right)$ by (8);
16   Update $\tilde{\mathcal{Q}}\left(\tilde{W}_j^t, S_j^t\right)$ by (43);
17   Update $\tilde{\pi}\left(\tilde{W}_j^t, S_j^t\right)$ by (44);

B. PHC-based VDD Size Strategy of UAV

The state vector $\tilde{W}_j^t$ observed by type-j UAV at t-th time slot contains the previous GCS's reward, i.e., $\tilde{W}_j^t = R_j^{t-1}$. Each UAV uniformly quantizes its contractual VDD size strategy into $B+1$ levels, i.e., $S_j \in \mathcal{B} = \{\frac{b}{B} \cdot S_{\max}\}_{0 \le b \le B}$. Let $\tilde{\mathcal{Q}}\left(\tilde{W}_j^t, S_j^t\right)$ denote the Q-function of type-j UAV. Similarly, the Q-function is updated by the iterative Bellman equation:

$$\tilde{\mathcal{Q}}\left(\tilde{W}_j^t, S_j^t\right) \leftarrow (1-\kappa_2)\tilde{\mathcal{Q}}\left(\tilde{W}_j^t, S_j^t\right) + \kappa_2 \left\{\mathcal{U}_j\left(\tilde{W}_j^t, S_j^t\right) \right.$$
$$\left. + \varphi_1 \max_{S_j} \tilde{\mathcal{Q}}\left(\tilde{W}_j^{t+1}, S_j^{t+1}\right)\right\}, \forall j \in \mathcal{J}', \quad (43)$$

where κ_2 is the learning rate, and φ_2 is the discount factor.

Similarly, the mixed-strategy table $\tilde{\pi}\left(\tilde{W}_j^t, S_j^t\right)$ of type-j UAV in PHC is updated by

$$\tilde{\pi}\left(\tilde{W}_j^t, S_j^t\right) \leftarrow \tilde{\pi}\left(\tilde{W}_j^t, S_j^t\right)$$
$$+ \begin{cases} \rho_2, & \text{if } S_j^t = \arg\max_{S_j} \tilde{\mathcal{Q}}\left(\tilde{W}_j^t, S_j\right); \\ -\frac{\rho_2}{B+1}, & \text{otherwise.} \end{cases} \quad (44)$$

Here, ρ_2 is a small positive value. According to the mixed-strategy table, each type-j UAV ($j \in \mathcal{J}'$) chooses its VDD size strategy S_j^t with the following chance:

$$\Pr\left(S_j^t = \hat{S}_j\right) = \pi\left(\tilde{W}_j^t, \hat{S}_j\right), \forall \hat{S}_j \in \mathcal{B}. \quad (45)$$

The hotbooting PHC-based optimal contractual VDD size strategy-making process of each type of UAV is summarized in lines 11–17 in Algorithm 2.

Remark. The above two-layer strategy-making process is repeated between the GCS and each type of UAV in $\mathcal{J}'$ until the strategies of both sides converge to stable values.

C. Hotbooting PHC for Practical Deployment

To speed up the convergence rate, a hotbooting technique is employed for both sides by learning from similar scenarios in an offline manner for efficient initialization of the Q-table and mixed-strategy table. Specifically, as shown in line 2 in Algorithm 2, by exploiting p numbers of historical interactions conducted in similar scenarios before the game starts, the hotbooting process outputs $\mathcal{Q}_p$ and $\tilde{\mathcal{Q}}_p$ as the initial Q-tables, and outputs π_p and $\tilde{\pi}_p$ as the initial mixed-strategy tables. Thereby, the inefficient random explorations in traditional PHC learning with all-zero initialization of Q-value and mixed-strategy table can be mitigated. The overall computational complexity of Algorithm 2 yields $\mathcal{O}(J' \times T_e)$, where T_e means the maximum interaction times and J' is the number of participating UAVs.

VIII. PERFORMANCE EVALUATION

This section first introduces the simulation setup, followed by the numerical results and discussions.

A. Simulation Setup

We consider a simulation area of $200 \times 200 \times 20\,\text{m}^3$ with one GCS and $I = 10$ uniformly distributed Parrot AR Drone 2.0 UAVs. Each UAV is embedded with a honeypot system and communicates with the GCS and other UAVs via Wi-Fi communications. Similar to the project HoneyDrone [14], the honeypot reads UAV profiles from the configuration file to emulate UAV's radio interfaces and offers low to medium interactions with adversaries for Wi-Fi protocols. The Telnet attack [14] is considered in the simulation, and the honeypot's captured VDD (including IP address, port number, connection type, commands, and timestamps of attackers) is recorded into a local MongoDB database. The GCS requests VDD from UAVs every 6 seconds, with a maximum communication delay of 2 seconds and a default system budget $\Omega = 460$. For simplicity, UAVs' types are assumed to be uniformly distributed. The lower and upper bounds of UAV's marginal VDD cost are set as 0.01 and 1, respectively. For the utility model, we set $\varpi = 6$, $C_0 = 1$, $\overline{R} = 480$, $T_{\max} = 2$ seconds, $S_{\max} = 300$ bytes. For the PHC learning, we set $\kappa_1 = \kappa_2 = 0.7$, $\varphi_1 = \varphi_2 = 0.8$, $\rho_1 = \rho_2 = 0.01$. Simulation parameters are summarized in Table II.

The following three conventional contract approaches are used for performance comparison with the proposed scheme.

- *Complete information contract.* In this ideal scenario, the GCS knows the private type of each UAV, and only IR constraints should be met in optimal contract design via Eqs. (21) and (22).
- *Linear contract.* The reward offered by the GCS is in direct proportion to UAV's shared VDD size in this contract, i.e., $R_j = \mu_G \times S_j$, $\forall j \in \mathcal{J}$, where μ_G is the unit payment per VDD size. Here, we set $\mu_G = \max\{C_j, \forall j \in \mathcal{J}'\}$, i.e., $\mu_G = C_1$.
- *Uniform contract.* In this contract, the GCS applies a single uniform contract item for all types of UAVs, i.e., $\Phi_j = \{S_1^*, R_1^*\}$, $\forall j \in \mathcal{J}$.

TABLE II
SIMULATION PARAMETERS

Param	Value	Param	Value
I	10	J	10
Z_i	$[30, 80]$ m	$V_{\max}^i$	20 m/s
$S_{\max}$	300 bytes	$T_{\max}$	2 seconds
C_0	1	C_j	$[0.01, 1]$
$\overline{R}$	480	D_G	800 bytes
ϖ	6	ι	2
κ_{LoS}	1	κ_{NLoS}	20
u_1	12	u_2	0.135
P_i^{Tr}	23 dBm	φ^2	−96 dBm
B^{U2C}	1 MHz	B^{U2U}	0.25 MHz
κ_1	0.7	κ_2	0.7
φ_1	0.8	φ_2	0.8
ρ_1	0.01	ρ_2	0.01

B. Numerical Results

We first evaluate the optimal contractual VDD size and contractual reward under different schemes in Figs. 2 and 3, followed by the contractual feasibility analysis of the proposed scheme in Fig. 4. Then, in Figs. 5–7, we evaluate and compare the utility of the UAV, the utility of the GCS, and the social surplus in different schemes. Next, the collaborative defensive effectiveness under different schemes is evaluated in Fig. 8. Finally, we evaluate UAV's VDD size strategy, GCS's reward strategy, and their utilities during the dynamic contractual strategy-making process based on PHC in Figs. 8–10. Here, the *defensive effectiveness* is defined as

$$\zeta = \frac{\sum_{j \in \mathcal{J}'} S_j}{D_G}, \tag{46}$$

where D_G is the VDD requirement of the GCS. Here, we set $D_G = 800$ bytes.

Figs. 2 and 3 show the optimal contractual VDD size and reward for different UAV types, respectively, in the optimal contract under partial information asymmetry. As seen in the two figures, with the increase of the marginal VDD cost of the UAV (i.e., the decrease of the type of UAV), both the optimal contractual VDD size and reward are in decline, which accords with the monotonicity constraints in Theorem 2. In addition, in the cases of information symmetry and information asymmetry, the optimal contractual VDD size is a convex function of the UAV type, which is consistent with the analysis in Theorems 1 and 4. In the linear contract, the optimal contractual VDD size and reward vary very little, given different UAV types. It is because the privacy information disclosure strategy is not implemented in the linear contract, and the degree of information asymmetry cannot be reduced, resulting in the unwillingness of UAVs to contribute more local honeypot data. In the uniform contract, when the UAV type changes, the optimal contractual VDD size and reward always remain the same. The reason is that the GCS only provides a single contract for all types of UAVs.

Fig. 4 evaluates the contractual feasibility in the proposed scheme under partial information asymmetry, by comparing the utilities of five different types of UAVs (i.e., types 1, 3, 5, 7, and 10) when selecting different contract items designed by the GCS. It can be seen that each UAV can obtain the maximum non-negative utility only when it truthfully selects the contract
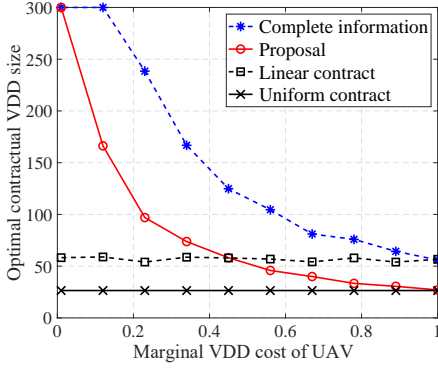
Fig. 2. Optimal contractual VDD size vs. marginal VDD cost of UAV in the proposed scheme under partial information asymmetry, compared with other three contract approaches.
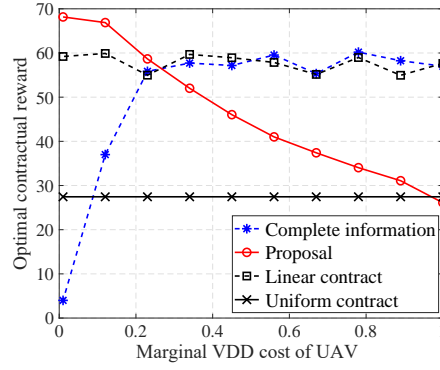

Fig. 3. Optimal contractual reward vs. marginal VDD cost of UAV in the proposed scheme under partial information asymmetry, compared with other three contract approaches.
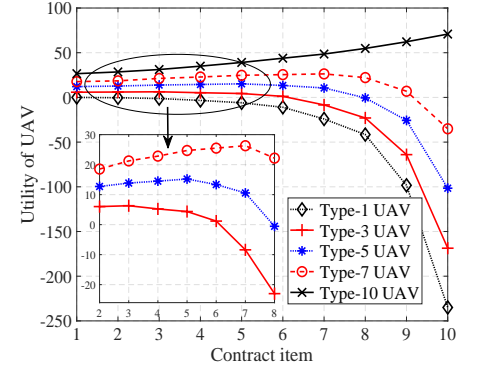

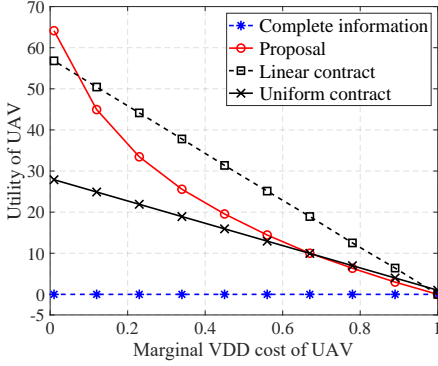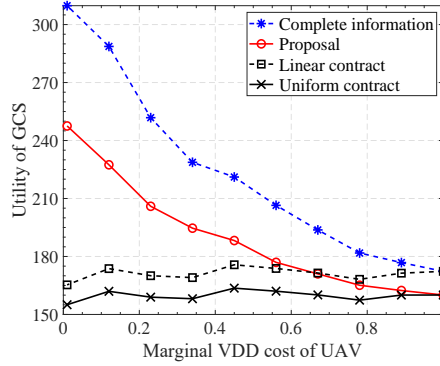Fig. 4. The utilities of different types of UAV when selecting different contract items in the optimal contract under partial information asymmetry.

Fig. 5. Utility of UAV vs. marginal VDD cost of UAV in the proposed scheme under partial information asymmetry, compared with other three contracts.

Fig. 6. Utility of GCS vs. marginal VDD cost of UAV in the proposed scheme under partial information asymmetry, compared with other three contracts.
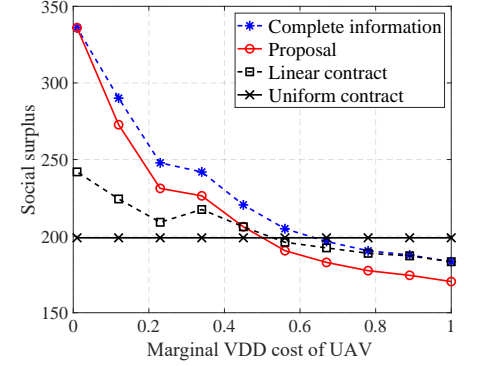

Fig. 7. Social surplus vs. marginal VDD cost of UAV in the proposed scheme under partial information asymmetry, compared with other three contracts.

designed for its type, which validates the contractual feasibility (i.e., IR and IC constraints) of the proposed optimal contract. In the proposed scheme, after each UAV truthfully chooses its contract item, the aggregated UAVs' true type information will be automatically revealed to the GCS (but the GCS still does not know that each UAV belongs to a certain type). That is to say, the optimal contract under information asymmetry enables the GCS to obtain more relevant information about UAVs' multi-dimensional private types, thereby reducing the degree of information asymmetry. In addition, in Fig. 4, when different types of UAVs select the same contract item, the higher the UAV type, the greater the UAV utility. It is because when UAVs choose the same contract item, the lower the marginal UAV cost (i.e., the higher type), the higher its corresponding utility. Besides, as seen in Fig. 4, the higher the UAV type, the higher the maximum UAV utility, which conforms to Corollary 2.

Fig. 5 shows the UAV utility in four schemes when UAV's marginal VDD cost varies between 0.01 and 1. As seen in Fig. 5, the UAV's utility remains zero under no information asymmetry. The reason is that the GCS intends to maximize its utility while enforcing IR, which is consistent with (21)–(22). Moreover, in Fig. 5, the lower type brings higher utility to the UAV, which conforms to the monotonicity of the optimal contract. Overall, our proposal attains higher utility for low-type UAVs (with higher marginal VDD cost) than the
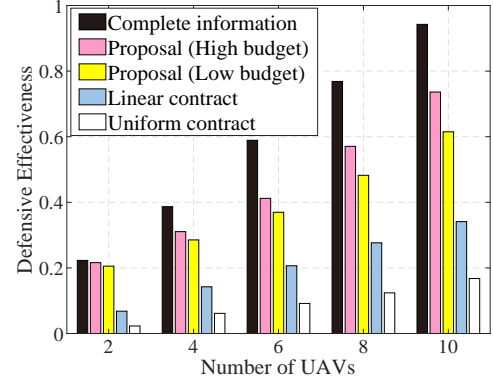

Fig. 8. Defensive effectiveness vs. number of UAV in the proposed scheme under partial information asymmetry, compared with other three contracts.

linear contract, and higher utility for high-type UAVs than the uniform contract.

Fig. 6 shows the utility of the GCS under different marginal VDD costs of UAV in different schemes. It can be seen that under the complete information, the GCS can obtain the highest utility among the four schemes, as the GCS fully knows the private types of all UAVs. Under the incomplete information, although the optimal contracts can motivate UAVs to select the contract items designed for their types truthfully, their true types are still unavailable to GCS. Therefore, the GCS
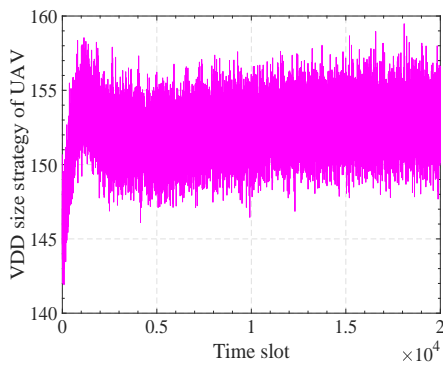
Fig. 9. Evolution of UAV's strategy on VDD size using PHC learning under complete information asymmetry.
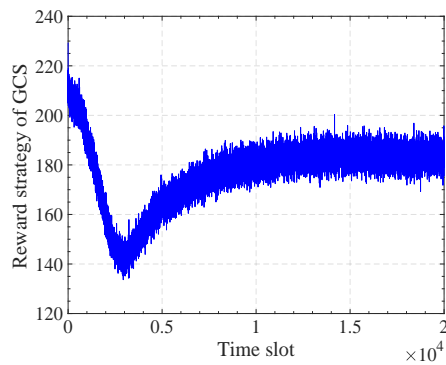

Fig. 10. Evolution of GCS's reward strategy using PHC learning under complete information asymmetry.
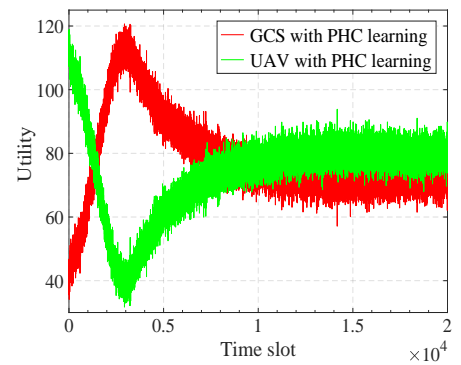

Fig. 11. Evolution of utilities of UAV and GCS using PHC learning under complete information asymmetry.

can only approach the socially optimal utility by designing optimal contracts in the case of information asymmetry, which is consistent with Corollary 1. Similar to the above analysis in Fig. 5, it can be seen from Fig. 6 that in the proposed contract scheme, higher UAV types (i.e., with lower marginal VDD cost) can bring higher benefits (i.e., higher utility) to the GCS. Besides, we can observe that in the proposed scheme under incomplete information, the utility of the GCS is higher than that in the uniform contract, and is higher than that in the linear contract for medium and high types of UAVs. It is because the uniform contract and linear contract have no restrictions on UAV's contract selection, and cannot motivate UAVs to exhibit their true private type information, making the GCS unable to obtain higher utility.

Fig. 7 shows the social surplus (i.e., the sum of utilities of UAVs and the GCS) in four schemes given different UAV's marginal VDD costs. As seen in Fig. 7, the utility of the UAV with the highest type (i.e., with the lowest VDD cost) in incomplete information is the same as that in the complete information, which accords with Theorems 1 and 3. For other UAV types under incomplete information, they can still obtain approximately optimal utility in the complete information. In the linear contract and uniform contract, the social surplus is generally low due to the inability to obtain additional UAV's private type information. In addition, in the uniform contract, since the GCS only provides a uniform contract item for all UAV types, the social surplus will not change when the UAV type varies.

Fig. 8 depicts the defensive effectiveness in four schemes given different number of participating UAVs. In this simulation, the budget is dynamically adjusted with the number of UAVs and two types of system budgets are adopted, i.e., high budget $\Omega_1 = \{160, 320, 480, 640, 800\}$ and low budget $\Omega_2 = \{92, 184, 276, 368, 460\}$. As shown in Fig. 8, our proposed scheme under partial information asymmetry outperforms both linear and uniform contracts in terms of higher defensive effectiveness, and its gap with the ideal complete information contract shrinks as the number of UAVs decreases. The reason is that the reward in the uniform contract and linear contract is either fixed or linear with the VDD. Notably, the relationship between the optimal reward and optimal VDD size in optimal contracts is nonlinear in our proposal, creating a stronger

incentive for UAVs to contribute more VDD and improve defensive effectiveness. Besides, in our proposal, the higher system budget results in better defensive performance. It can be explained as follows. According to Lemma 2, the GCS tends to exhaust the available budget. Moreover, according to Theorem 4, a higher budget can incentivize UAVs' high amount of contributed VDD, thereby leading to improved defensive effectiveness.

Next, in Figs. 9–11, we show the convergence of PHC-based optimal dynamic contract for a randomly selected UAV under complete information asymmetry. The evolutions of UAV's VDD size strategy and GCS's reward strategy via PHC learning are shown in Fig. 9 and Fig. 10, respectively. The evolutions of average utilities of the UAV and the GCS in PHC learning are shown in Fig. 11. As seen in these three figures, both the VDD size and reward in dynamic contracts can converge to stable and optimal values, validating the feasibility of the proposed two-layer PHC learning-based incentive mechanism. In Fig. 9, the VDD size first increases then converges to a stable state, while the corresponding contractual reward in Fig. 10 first decreases then grows to reach the stable state. In Fig. 11, the utility of UAV first decreases then grows to reach the stable value, while the utility of GCS first increases then gradually drops to the convergent value. The reasons are as follows. Motivated by the initial high reward of the GCS, the UAV intends to share more VDD to improve its utility. Then, after observing UAV's high VDD contribution, the GCS gradually decreases its reward to increase its utility. After that, the UAV and GCS continuously pursue their maximized utilities by seeking the optimal VDD size and reward strategy based on their observed system states.

IX. CONCLUSION

In this paper, we have proposed an optimal and feasible incentive mechanism to promote collaborative defense for UAVs by sharing their captured VDD in local honeypots. Firstly, a novel honeypot game has been formulated between the GCS and UAVs with distinct types (i.e., VDD cost and communication delay), the solution of which is to design optimal VDD-reward contracts under both partial and complete information asymmetry scenarios. Secondly, we have analytically derived the optimal contracts with budget and contract feasibility under

partial information asymmetry, by summarizing UAV's multi-dimensional private information into a one-dimensional metric. Thirdly, a two-layer PHC learning algorithm has been devised to intelligently address the dynamic contract design problem under complete information asymmetry and time-varying UAV networks. Numerical results have demonstrated that the proposed scheme can effectively encourage UAVs to share local VDD with the GCS and effectively enhance UAV's utility and collaborative defensive performance under both partial and complete information asymmetry. For future work, we plan to investigate the federated learning approaches for privacy-preserving honeypot data sharing and defense service offerings among UAVs. Besides, the trust-free honeypot data sharing based on lightweight blockchain will be further studied.

REFERENCES

[1] H. Wang, H. Zhao, J. Zhang, D. Ma, J. Li, and J. Wei, "Survey on unmanned aerial vehicle networks: A cyber physical system perspective," *IEEE Communications Surveys & Tutorials*, vol. 22, no. 2, pp. 1027–1070, 2020.

[2] Y. Wang, W. Chen, T. H. Luan, Z. Su, Q. Xu, R. Li, and N. Chen, "Task offloading for post-disaster rescue in unmanned aerial vehicles networks," *IEEE/ACM Transactions on Networking*, vol. 30, no. 4, pp. 1525–1539, 2022.

[3] J. Gao, Z. Hu, K. Bian, X. Mao, and L. Song, "AQ360: UAV-aided air quality monitoring by 360-degree aerial panoramic images in urban areas," *IEEE Internet of Things Journal*, vol. 8, no. 1, pp. 428–442, 2021.

[4] T. Do-Duy, L. D. Nguyen, T. Q. Duong, S. R. Khosravirad, and H. Claussen, "Joint optimisation of real-time deployment and resource allocation for UAV-aided disaster emergency communications," *IEEE Journal on Selected Areas in Communications*, vol. 39, no. 11, pp. 3411–3424, 2021.

[5] Z. Su, Y. Wang, Q. Xu, and N. Zhang, "LVBS: Lightweight vehicular blockchain for secure data sharing in disaster rescue," *IEEE Transactions on Dependable and Secure Computing*, vol. 19, no. 1, pp. 19–32, 2022.

[6] Z. Chen, J. Tian, H. Liu, J. Yu, and X. Chen, "Novel pattern-diverse millimeter-wave antenna with broadband, high-gain, enhanced-coverage for energy-efficient unmanned aerial vehicle," *IEEE Transactions on Vehicular Technology*, vol. 70, no. 5, pp. 4081–4087, 2021.

[7] A. Eldosouky, A. Ferdowsi, and W. Saad, "Drones in distress: A game-theoretic countermeasure for protecting UAVs against GPS spoofing," *IEEE Internet of Things Journal*, vol. 7, no. 4, pp. 2840–2854, 2020.

[8] E. D. Saputro, Y. Purwanto, and M. F. Ruriawan, "Medium interaction honeypot infrastructure on the internet of things," in *IEEE International Conference on Internet of Things and Intelligence System (IoTaIS)*, 2021, pp. 98–102.

[9] Z. Zhan, M. Xu, and S. Xu, "Characterizing honeypot-captured cyber attacks: Statistical framework and case study," *IEEE Transactions on Information Forensics and Security*, vol. 8, no. 11, pp. 1775–1789, 2013.

[10] N. Garg and D. Grosu, "Deception in honeynets: A game-theoretic analysis," in *IEEE SMC Information Assurance and Security Workshop*, 2007, pp. 107–113.

[11] J. You, S. Lv, Y. Sun, H. Wen, and L. Sun, "HoneyVP: A cost-effective hybrid honeypot architecture for industrial control systems," in *IEEE International Conference on Communications (ICC)*, 2021, pp. 1–6.

[12] B. Wang, Y. Dou, Y. Sang, Y. Zhang, and J. Huang, "IoTCMal: Towards a hybrid IoT honeypot for capturing and analyzing malware," in *IEEE International Conference on Communications (ICC)*, 2020, pp. 1–7.

[13] E. Vasilomanolakis, S. Karuppayah, M. Mühlhäuser, and M. Fischer, "HosTaGe: A mobile honeypot for collaborative defense," in *International Conference on Security of Information and Networks*, 2014, pp. 330–333.

[14] J. Daubert, D. Boopalan, M. Mühlhäuser, and E. Vasilomanolakis, "HoneyDrone: A medium-interaction unmanned aerial vehicle honeypot," in *IEEE/IFIP Network Operations and Management Symposium (NOMS)*, 2018, pp. 1–6.

[15] W. Tian, M. Du, X. Ji, G. Liu, Y. Dai, and Z. Han, "Honeypot detection strategy against advanced persistent threats in industrial internet of things: A prospect theoretic game," *IEEE Internet of Things Journal*, vol. 8, no. 24, pp. 17 372–17 381, 2021.

[16] K. Wang, M. Du, S. Maharjan, and Y. Sun, "Strategic honeypot game model for distributed denial of service attacks in the smart grid," *IEEE Transactions on Smart Grid*, vol. 8, no. 5, pp. 2474–2482, 2017.

[17] W. Tian, M. Du, X. Ji, G. Liu, Y. Dai, and Z. Han, "Contract-based incentive mechanisms for honeypot defense in advanced metering infrastructure," *IEEE Transactions on Smart Grid*, vol. 12, no. 5, pp. 4259–4268, 2021.

[18] Q. D. La, T. Q. S. Quek, J. Lee, S. Jin, and H. Zhu, "Deceptive attack and defense game in honeypot-enabled networks for the internet of things," *IEEE Internet of Things Journal*, vol. 3, no. 6, pp. 1025–1035, 2016.

[19] O. Tsemogne, Y. Hayel, C. Kamhoua, and G. Deugoué, "Game-theoretic modeling of cyber deception against epidemic botnets in internet of things," *IEEE Internet of Things Journal*, vol. 9, no. 4, pp. 2678–2687, 2022.

[20] O. A. Wahab, J. Bentahar, H. Otrok, and A. Mourad, "Resource-aware detection and defense system against multi-type attacks in the cloud: Repeated bayesian stackelberg game," *IEEE Transactions on Dependable and Secure Computing*, vol. 18, no. 2, pp. 605–622, 2021.

[21] W. Fan, Z. Du, M. Smith-Creasey, and D. Fernández, "HoneyDOC: An efficient honeypot architecture enabling all-round design," *IEEE Journal on Selected Areas in Communications*, vol. 37, no. 3, pp. 683–697, 2019.

[22] A. M. Zarca, J. B. Bernabe, A. Skarmeta, and J. M. Alcaraz Calero, "Virtual IoT honeynets to mitigate cyberattacks in SDN/NFV-enabled IoT networks," *IEEE Journal on Selected Areas in Communications*, vol. 38, no. 6, pp. 1262–1277, 2020.

[23] Z. Zhou, J. Feng, B. Gu, B. Ai, S. Mumtaz, J. Rodriguez, and M. Guizani, "When mobile crowd sensing meets UAV: Energy-efficient task assignment and route planning," *IEEE Transactions on Communications*, vol. 66, no. 11, pp. 5526–5538, 2018.

[24] M. M. Azari, G. Geraci, A. Garcia-Rodriguez, and S. Pollin, "UAV-to-UAV communications in cellular networks," *IEEE Transactions on Wireless Communications*, vol. 19, no. 9, pp. 6130–6144, 2020.

[25] Y. Zeng, J. Xu, and R. Zhang, "Energy minimization for wireless communication with rotary-wing UAV," *IEEE Transactions on Wireless Communications*, vol. 18, no. 4, pp. 2329–2345, 2019.

[26] X. Li, H. Yao, J. Wang, X. Xu, C. Jiang, and L. Hanzo, "A near-optimal UAV-aided radio coverage strategy for dense urban areas," *IEEE Transactions on Vehicular Technology*, vol. 68, no. 9, pp. 9098–9109, 2019.

[27] Q. Xu, Z. Su, and R. Lu, "Game theory and reinforcement learning based secure edge caching in mobile social networks," *IEEE Transactions on Information Forensics and Security*, vol. 15, pp. 3415–3429, 2020.

[28] Y. Wang, Z. Su, N. Zhang, and A. Benslimane, "Learning in the air: Secure federated learning for UAV-assisted crowdsensing," *IEEE Transactions on Network Science and Engineering*, vol. 8, no. 2, pp. 1055–1069, 2021.

[29] L. Gao, X. Wang, Y. Xu, and Q. Zhang, "Spectrum trading in cognitive radio networks: A contract-theoretic modeling approach," *IEEE Journal on Selected Areas in Communications*, vol. 29, no. 4, pp. 843–855, 2011.

[30] P. Bolton and M. Dewatripont, *Contract Theory*. Cambridge, MA, USA: MIT Press, 2005.

[31] Y. Chen, X. Tian, Q. Wang, J. Jiang, M. Li, and Q. Zhang, "SAFE: A general secure and fair auction framework for wireless markets with privacy preservation," *IEEE Transactions on Dependable and Secure Computing*, vol. 19, no. 3, pp. 2038–2053, 2022.

APPENDIX A
PROOF OF LEMMA 1

Proof: Obviously, the optimal payment reward for the GCS is zero for non-participating UAVs. For the optimal rewards of participating UAVs, we prove it by contradiction. Suppose that there exists an optimal reward policy $\hat{R}_j$ that satisfies $\hat{R}_j - C_j S_j - C_0 \neq 0$. First, we assume that the optimal reward policy satisfies $\hat{R}_j - C_j S_j - C_0 < 0$, which contradicts the IR constraint. Second, we suppose it satisfies $\hat{R}_j - C_j S_j - C_0 > 0$. Since the utility of the GCS decreases as the payment reward increases, the GCS can continuously increase its utility by reducing the reward $\hat{R}_j$ until $\hat{R}_j - C_j S_j - C_0 = 0$, which contradicts the assumption that $\hat{R}_j - C_j S_j - C_0 > 0$. To sum up, there exists no optimal reward strategy $\hat{R}_j$ that satisfies $\hat{R}_j - C_j S_j - C_0 \neq 0$. ∎

APPENDIX B
PROOF OF LEMMA 2

Proof: Suppose that $\sum_{j=1}^{J'} N_j R_j < \Omega$. Then, the GCS could always prefer a larger R_j, which allows for a larger VDD size S_j from type-j UAV, to enhance the defensive performance until $\sum_{j=1}^{J'} N_j R_j = \Omega$. ∎

APPENDIX C
PROOF OF THEOREM 1

Proof: Obviously, for any non-participating UAV ($\forall j \notin \mathcal{J}'$), the optimal contract VDD size and payment reward are both zero. For any participating UAV ($\forall j \in \mathcal{J}'$), as $\frac{\partial^2 \mathscr{L}(S_j, \lambda_1)}{\partial S_j^2} = -\frac{\varpi N_j}{T_j(1+S_j)^2} < 0$, it indicates that $\mathscr{L}(S_j, \lambda_1)$ is a strictly convex function about S_j. Therefore, the optimal contractual VDD size S_j^* can be found at the point $\frac{\partial \mathscr{L}(S_j, \lambda_1)}{\partial S_j} = 0$ and $\frac{\partial \mathscr{L}(S_j, \lambda_1)}{\partial \lambda_1} = 0$ at or at the boundary point.

Let $\frac{\partial \mathscr{L}(S_j, \lambda_1)}{\partial S_j} = 0$ and $\frac{\partial \mathscr{L}(S_j, \lambda_1)}{\partial \lambda_1} = 0$, after some derivations and simple transformations, we can obtain

$$\tilde{S}_j^* = \frac{1}{T_j C_j} \cdot \frac{\Omega - \sum_{j=1}^{J'} N_j(C_0 - C_j)}{\sum_{j=1}^{J'} \frac{N_j}{T_j}} - 1$$
$$= \frac{\Lambda}{T_j C_j} - 1. \tag{47}$$

Hence, $S_j^* = \min\left\{S_{\max}, \max\left\{\tilde{S}_j^*, 0\right\}\right\}$. According to (16) in Lemma 1, the corresponding optimal reward can be derived, as shown in (22). ∎

APPENDIX D
PROOF OF THEOREM 2

Proof: Obviously, in case 1 (i.e., $j \notin \mathcal{J}'$), the corresponding contractual VDD size and reward are zero (i.e., $S_j = R_j = 0$). Thereinafter, we focus on the case 2 (i.e., $j \in \mathcal{J}'$) for UAV types that can timely transmit their VDD to the GCS. As the contractual feasibility means that both IR and IC constraints are satisfied, we need to prove the equivalence between the constraints (26)–(28) and the IR&IC constraints in (13)–(14).

1) Necessity: We need to prove that if IR and IC constraints hold for all types of UAVs, then the constraints (26)–(28) automatically hold.

(i) According to IR constraint for type-1 UAV, we have $R_1 - C_1 S_1 - C_0 \geq 0$, which is shown in (27).

(ii) According to IC constraints for type-j and type-k UAVs ($j \neq k$), we have

$$R_j - C_j S_j \geq R_k - C_j S_k, \tag{48}$$

$$R_k - C_k S_k \geq R_j - C_k S_j. \tag{49}$$

Combining the above two constraints, we can derive $(C_j - C_k)(S_j - S_k) \leq 0$. As $C_1 > C_2 > \cdots > C_{J'}$ and $S_j \geq 0$, we have $0 \leq S_1 \leq S_2 \leq \cdots \leq S_{J'}$. Besides, based on (48), we have

$$C_j(S_j - S_k) \leq R_j - R_k \leq C_k(S_j - S_k), \tag{50}$$

which leads to $0 \leq R_1 \leq R_2 \leq \cdots \leq R_{J'}$. Hence, we obtain the monotonicity constraint (26).

(iii) Considering IC constraints for two neighboring contract items, we have

$$R_j - C_j S_j \geq R_{j-1} - C_j S_{j-1}, \tag{51}$$

$$R_{j-1} - C_{j-1} S_{j-1} \geq R_j - C_{j-1} S_j. \tag{52}$$

Combining the above two constraints, we can obtain $C_j(S_j - S_{j-1}) \leq R_j - R_{j-1} \leq C_{j-1}(S_j - S_{j-1})$, which is shown in (28).

To summarize, (26)–(28) are the necessity conditions of IR and IC constraints.

2) Sufficiency: We prove by mathematical induction that if the constraints (26)–(28) hold, then both IR and IC constraints are met for all UAV types. Let $\mathcal{A}(q)$ denote a subset of Φ, which consists of the first q contract items in Φ, i.e., $\mathcal{A}(q) = \{(S_j, R_j)|j = 1, 2, \cdots, q\}$. Let $\mathcal{J}(q) = \{1, 2, \cdots, q\}$. When $q = 1$, as there exists only one UAV type, only the IR constraint needs to be considered for a feasible contract. Obviously, according to (27), we have $R_1 - C_1 S_1 - C_0 \geq 0$. Then, $\mathcal{A}(1)$ is proved to be feasible.

Next, we show that if $\mathcal{A}(q)$ is feasible, $\mathcal{A}(q + 1)$ is also feasible. To achieve this goal, we need to prove the following two aspects. (i) Both the IR and IC constraints are met for the new type $q + 1$, i.e.,

$$\begin{cases} R_{q+1} - C_{q+1} S_{q+1} \geq 0, & (53) \\ R_{q+1} - C_{q+1} S_{q+1} \geq R_j - C_{q+1} S_j, \forall j \in \mathcal{J}(q). & (54) \end{cases}$$

And (ii) for all existing UAV types $j \in \mathcal{J}(q)$, IC constraints are met in the existence of type $q + 1$, i.e.,

$$R_j - C_j S_j \geq R_{q+1} - C_j S_{q+1}, \forall j \in \mathcal{J}(q). \tag{55}$$

Proof of part (i): Due to the feasibility of $\mathcal{A}(q)$, the IC constraint for type-q UAV is satisfied for any $k \in \mathcal{A}(q)$:

$$R_q - C_q S_q \geq R_k - C_q S_k. \tag{56}$$

According to the left part of constraint (28), we can attain

$$R_{q+1} \geq R_q + C_{q+1}(S_{q+1} - S_q). \tag{57}$$

Combining the above two inequalities, we can obtain

$$R_{q+1} - C_{q+1} S_{q+1} \geq R_q - C_{q+1} S_q$$
$$\geq R_k - C_{q+1} S_q + C_q(S_q - S_k)$$
$$\geq R_k - C_{q+1} S_q + C_{q+1}(S_q - S_k)$$
$$= R_k - C_{q+1} S_k, \forall k \in \mathcal{A}(q). \tag{58}$$

Thereby, the IC constraint is satisfied for type-$(q + 1)$ UAV.

As IR constraints hold for all type-k UAVs, we can further obtain $R_k - C_k S_k - C_0 \geq 0, \forall k \in \mathcal{A}(q)$. Beside, since $k < q + 1$, we have $C_k > C_{q+1}$. As such, we have

$$R_{q+1} - C_{q+1} S_{q+1} \geq R_k - C_{q+1} S_k$$
$$\geq R_k - C_k S_k, \forall k \in \mathcal{A}(q)$$
$$\geq 0. \tag{59}$$

According to (59), the IR constraint is satisfied for type-$(q+1)$ UAV. Hence, part (i) is proved.

Proof of part (ii): Since $\mathcal{A}(q)$ is feasible, the IC constraint holds $\forall k \in \mathcal{A}(q)$:

$$R_k - C_k S_k \geq R_q - C_k S_q. \tag{60}$$

According to the right part of constraint (28), we can attain

$$R_{q+1} \leq R_q + C_q(S_{q+1} - S_q). \tag{61}$$

Combining the above two inequalities, we can obtain

$$\begin{aligned}
R_k - C_k S_k &\geq R_{q+1} - C_k S_q - C_q(S_{q+1} - S_q) \\
&\geq R_{q+1} - C_k S_q - C_k(S_{q+1} - S_q) \\
&= R_{q+1} - C_k S_{q+1}, \forall k \in \mathcal{A}(q). \tag{62}
\end{aligned}$$

Hence, part (ii) is proved. In summary, we have proved that (a) $\mathcal{A}(1)$ is feasible, and (b) if $\mathcal{A}(q)$ is feasible, $\mathcal{A}(q+1)$ is also feasible. Based on the mathematical induction method, it can be concluded that $\mathcal{A} = \mathcal{A}(J')$ is feasible. Theorem 2 is proved. ∎

APPENDIX E
PROOF OF THEOREM 3

Proof: Obviously, in case 1, for UAVs in $\mathcal{J}\backslash\mathcal{J}'$, the optimal contractual reward equals to zero. In what follows, we prove the case 2 by contradiction for UAVs in $\mathcal{J}'$.

1) Optimality: Notably, the reward strategy in (31) meets the constraints (12) and (13) in Theorem 1, and it satisfies the monotonicity constraint in (11) under the monotonic VDD size strategy. Here, we prove that the reward strategy in (31) maximizes the GCS's utility. Given the fixed VDD size strategy $\mathcal{S}$, the maximum utility of the GCS in (6) can be acquired by minimizing the $\sum_{j=1}^{J'} N_j R_j$. Suppose that there exists a reward sequence $\widehat{\mathbf{R}} = \{\hat{R}_j\}_{j\in\mathcal{J}'}$ such that $\sum_{j=1}^{J'} N_j \hat{R}_j < \sum_{j=1}^{J'} N_j R_j^*$. As a consequence, there exists at least one reward $\hat{R}_j < R_j^*$. According to Theorem 1, to ensure the contractual feasibility, $\widehat{\mathbf{R}}$ should satisfy:

$$\hat{R}_{j-1} + C_j(S_j - S_{j-1}) \leq \hat{R}_j < R_j^*. \tag{63}$$

According to (31), the above inequality in (63) can be reformulated as:

$$\hat{R}_{j-1} < R_j^* - C_j(S_j - S_{j-1}) = R_{j-1}^*. \tag{64}$$

Continuing the above process until $j = 1$, we can eventually obtain that $\hat{R}_1 < R_1^* = C_1 S_1 + C_0$, which violates the IR constraint for type-1 UAVs. Thereby, there does not exist any feasible reward strategy $\widehat{\mathbf{R}}$, and the utility of the GCS is optimized by applying the reward strategy in (31).

2) Uniqueness: To prove the uniqueness of the optimal reward strategy in (31), we first assume that there exists a reward strategy $\widehat{\mathbf{R}} = \{\hat{R}_j\}_{j\in\mathcal{J}'} \neq \mathbf{R}^*$ such that $\sum_{j=1}^{J'} N_j \hat{R}_j = \sum_{j=1}^{J'} N_j R_j^*$. Hence, there must exist at least one reward $\hat{R}_j \neq R_j^*$. Without loss of generality, it is assumed that $\hat{R}_j > R_j^*$. As such, there must exist another reward $\hat{R}_k < R_k^*$. Using the same method, we obtain a contradiction, which implies that the optimal reward strategy in (31) is unique. Theorem 3 is proved. ∎

APPENDIX F
PROOF OF THEOREM 4

Proof: By substituting the optimal reward strategy $R_j^*(\mathbf{S})$ in (33) into the BF constraint C4 in (32), we have

$$\begin{aligned}
\Omega &= \sum_{j\in\mathcal{J}'} N_j R_j^* = N_1 R_1^* + \sum_{j=2}^{J'} N_j R_j^* \\
&= \sum_{j=1}^{J'} N_j C_j S_j + \sum_{j=2}^{J'} N_j \sum_{k=1}^{j-1} (C_k - C_{k+1}) S_k + \sum_{j=1}^{J'} N_j C_0 \\
&= \sum_{j=1}^{J'} N_j C_j S_j + \sum_{j=1}^{J'-1} (C_j - C_{j+1}) S_j \sum_{k=j+1}^{J'} N_k + \sum_{j=1}^{J'} N_j C_0 \\
&= \sum_{j=1}^{J'} N_j C_j S_j + \sum_{j=1}^{J'-1} \Delta C_j S_j \sum_{k=j+1}^{J'} N_k + \sum_{j=1}^{J'} N_j C_0 \\
&= \sum_{j=1}^{J'} \left(A_j S_j + N_j C_0 \right). \tag{65}
\end{aligned}$$

Besides, the GCS's utility function $\mathcal{U}_G(\Phi)$ in (6) can be rewritten as

$$\mathcal{U}_G(\Phi) = \mathcal{U}_G(S_j) = \sum_{j\in\mathcal{J}'} \varpi \frac{N_j}{T_j} \log(1+S_j) - \Omega. \tag{66}$$

Hence, for the relaxed Problem 2-1 without the monotonicity constraint C1, the corresponding Lagrangian function can be expressed as:

$$\begin{aligned}
\mathscr{L}(S_j, \lambda_2) &= \mathcal{U}_G(S_j) + \lambda_2 \Big(\sum_{j=1}^{J'} \left(A_j S_j + N_j C_0 \right) - \Omega \Big) \\
&= \sum_{j=1}^{J'} \frac{\varpi N_j}{T_j} \log(1+S_j) + \lambda_2 \sum_{j=1}^{J'} \left(A_j S_j + N_j C_0 \right) \\
&\quad - (\lambda_2 + 1)\Omega, \tag{67}
\end{aligned}$$

where λ_2 represents the Lagrange multiplier.

As $\frac{\partial^2 \mathscr{L}(S_j, \lambda_2)}{\partial S_j^2} = -\frac{\varpi N_j}{T_j(1+S_j)^2} < 0$, $\mathscr{L}(S_j, \lambda_2)$ is strictly concave with respect to S_j. Thereby, the optimal VDD size strategy S_j^* can be obtained by

$$S_j^* = \min\left\{ S_{\max}, \max\left\{ \tilde{S}_j^*, 0 \right\} \right\}, \tag{68}$$

where the point $\tilde{S}_j^*$ simultaneously satisfies $\frac{\partial \mathscr{L}(S_j, \lambda_2)}{\partial S_j} = 0$ and $\frac{\partial \mathscr{L}(S_j, \lambda_2)}{\partial \lambda_2} = 0$. After some derivations and simple transformations, we can obtain

$$\begin{aligned}
\tilde{S}_j^* &= \frac{N_j}{A_j T_j} \cdot \frac{\Omega + \sum_{j=1}^{J'} A_j - C_0 \sum_{j=1}^{J'} N_j}{\sum_{j=1}^{J'} \frac{N_j}{T_j}} - 1 \\
&= \frac{N_j}{A_j T_j} \cdot \mathfrak{R} - 1. \tag{69}
\end{aligned}$$

Theorem 4 is proved. ∎